

Supplement of Hydrol. Earth Syst. Sci., 25, 957–982, 2021
<https://doi.org/10.5194/hess-25-957-2021-supplement>
© Author(s) 2021. This work is distributed under
the Creative Commons Attribution 4.0 License.



Supplement of

Learning from satellite observations: increased understanding of catchment processes through stepwise model improvement

Petra Hulsman et al.

Correspondence to: Petra Hulsman (p.hulsman@tudelft.nl)

The copyright of individual parts of the supplement might differ from the CC BY 4.0 License.

Supplements

- S1. Model performance with respect to all discharge signatures 2
- S2. Parameter sets selected based on discharge 3
 - S2.1 Time series: Discharge 3
 - S2.2. Time series: Evaporation (Basin average) 4
 - S2.3 Time series: Evaporation (Wetland dominated areas) 5
 - S2.4 Time series: Total water storage (Basin average) 6
 - S2.5. Spatial pattern: Evaporation (normalised, dry season) 7
 - S2.6. Spatial pattern: Total water storage (normalised, dry season) 8
- S3. Parameter sets selected based on multiple variables 10
 - S3.1. Time series: Evaporation (Basin average) 10
 - S3.2. Time series: Total water storage (Basin average) 11
 - S3.3. Spatial pattern: Evaporation (normalised, dry season) 12
 - S3.4. Spatial pattern: Total water storage (normalised, dry season) 13
- S4. Remaining graphs 14

S1. Model performance with respect to all discharge signatures

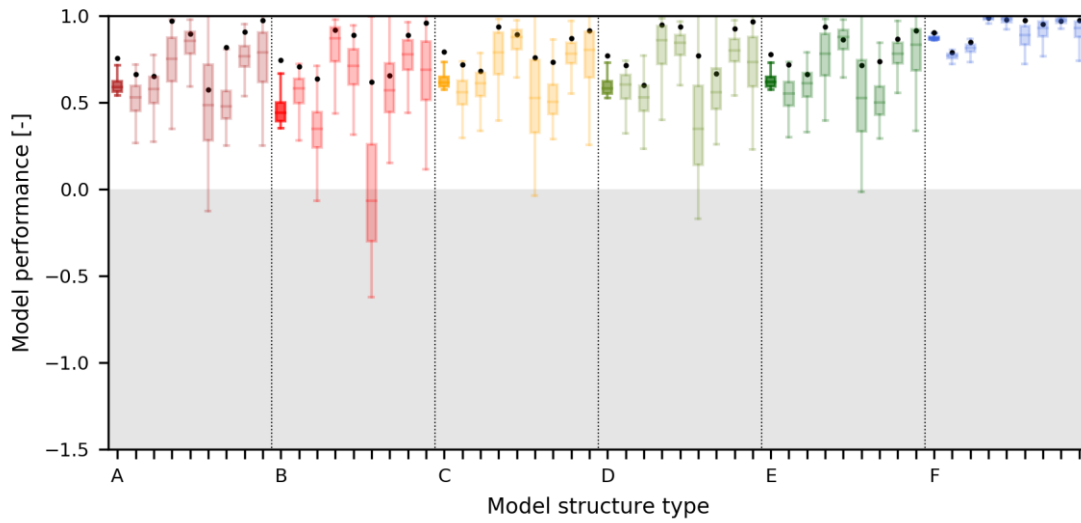


Figure S1: Calibrated model performance of all models with respect to discharge (2002 – 2012). The boxplots visualise the spread of the best 5% solutions according to $D_{E,Qcal}$ in the overall model performance $D_{E,Qcal}$ and the following individual signatures: 1) daily discharge ($E_{NS,Q}$), 2) its logarithm ($E_{NS,\log Q}$), 3) flow duration curve ($E_{NS,FDC}$), 4) its logarithm ($E_{NS,\log FDC}$), 5) average runoff coefficient during the dry season ($E_{R,RCdry}$), 6) average seasonal runoff coefficient during the wet season ($E_{R,RCwet}$), 7) autocorrelation function ($E_{NS,AC}$), and 8) rising limb density ($E_{R,RLD}$). The dots visualise the model performance with the “optimal” parameter set using the overall model performance metric ($D_{E,Qcalopt}$).

S2. Parameter sets selected based on discharge

S2.1 Time series: Discharge

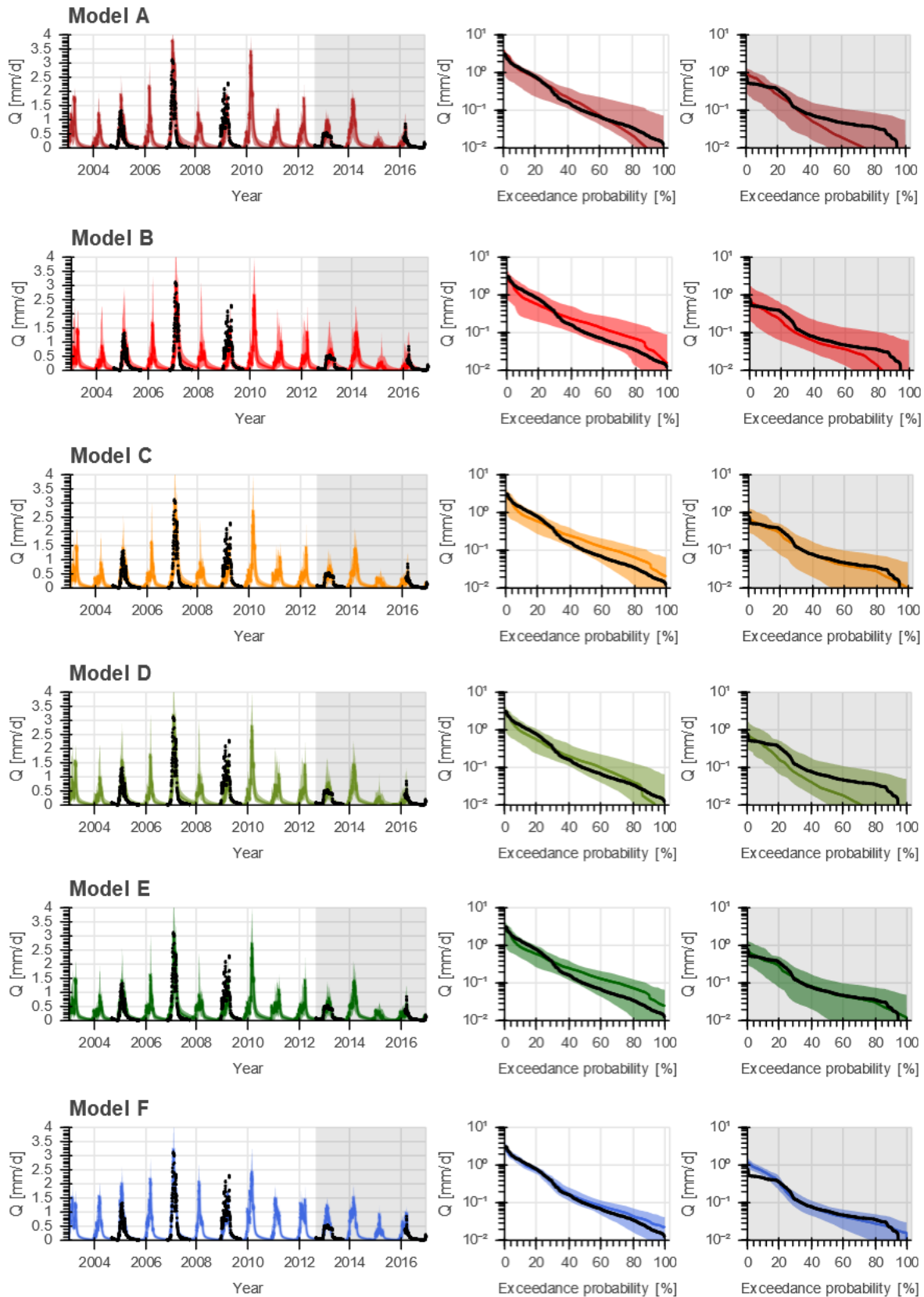


Figure S2: Range of model solutions for Models A to F. The left panel shows the hydrograph and the right panel the flow duration curve of the recorded (black) and modelled discharge: the line indicates the solution with the highest calibration objective function with respect to discharge ($D_{E, Q_{\text{cal}}}$) and the shaded area the envelope of the solutions retained as feasible. The data in the white area were used for calibration and the grey shaded area for validation.

S2.2. Time series: Evaporation (Basin average)

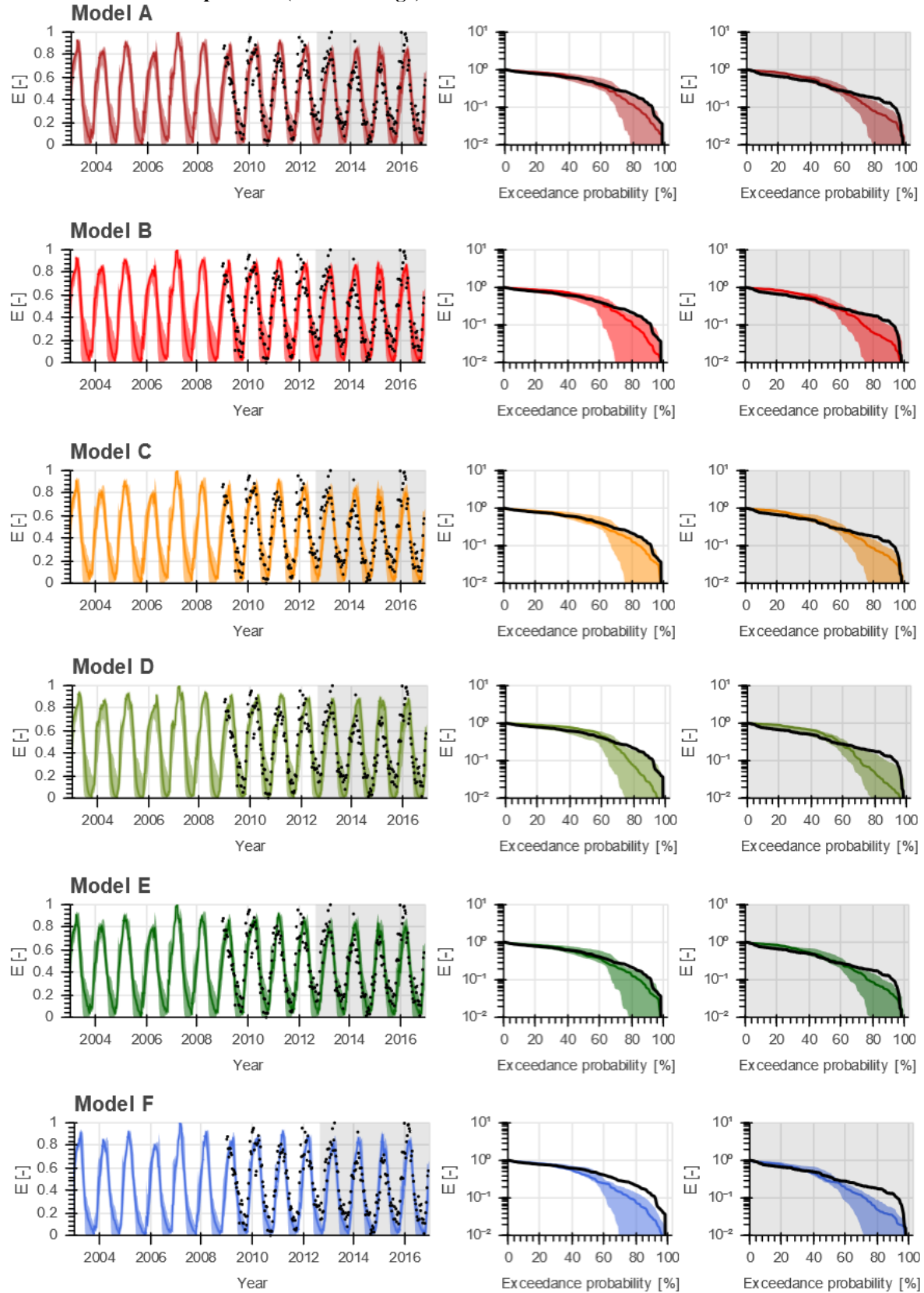


Figure S3: Range of model solutions for Models A to F. The left panel shows the time series and the right panel the duration curve of the recorded (black) and modelled normalised basin average evaporation: the line indicates the solution with the highest calibration objective function with respect to discharge ($D_{E,Q_{cal}}$) and the shaded area the envelope of the solutions retained as feasible. The data in the grey shaded area were used for validation.

S2.3 Time series: Evaporation (Wetland dominated areas)

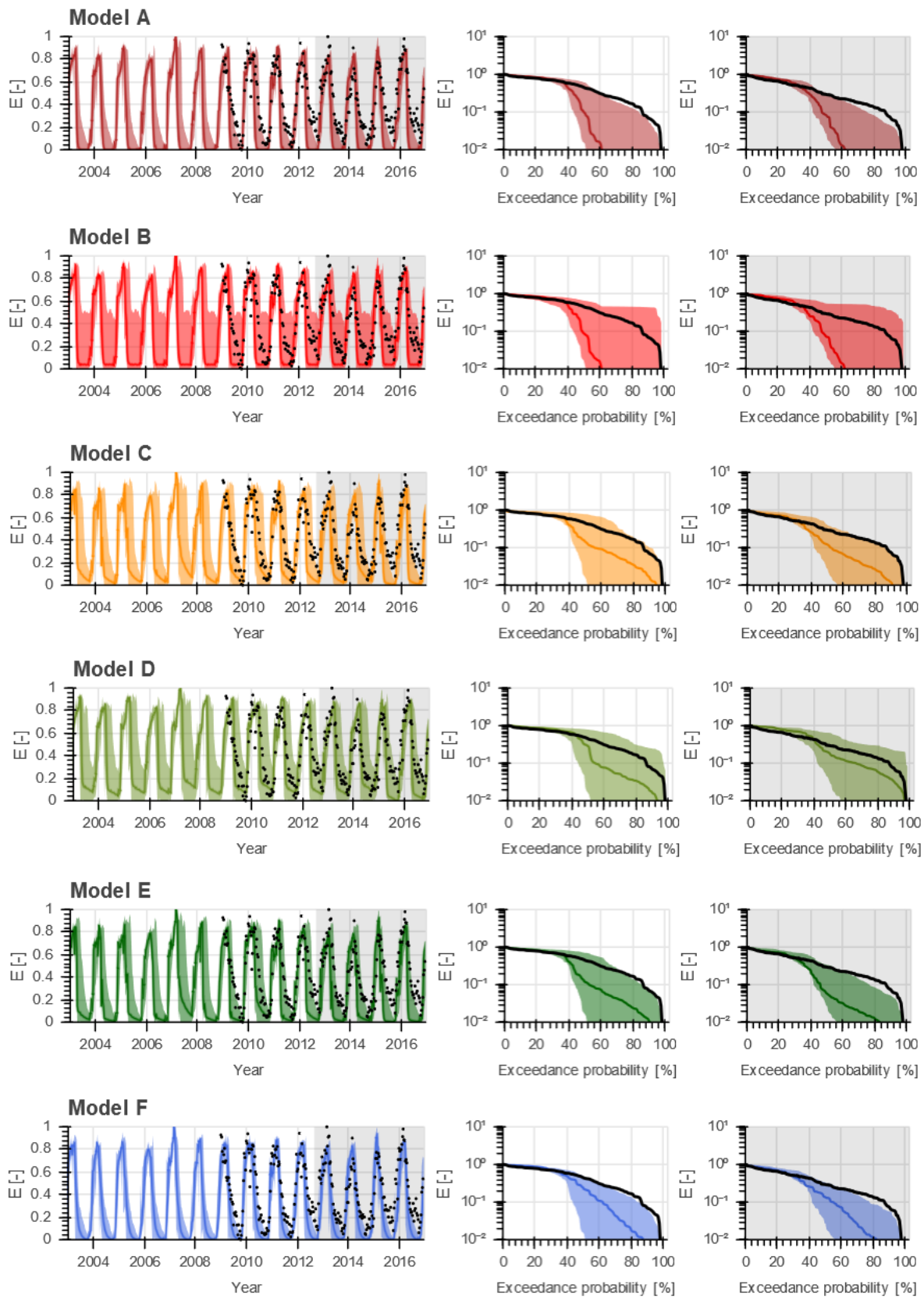


Figure S4: Range of model solutions for Models A to F. The left panel shows the time series and the right panel the duration curve of the recorded (black) and modelled normalized evaporation for wetland dominated areas: the line indicates the solution with the highest calibration objective function with respect to discharge ($D_{E,Q_{cal}}$) and the shaded area the envelope of the solutions retained as feasible. The data in the grey shaded area were used for validation.

S2.4 Time series: Total water storage (Basin average)

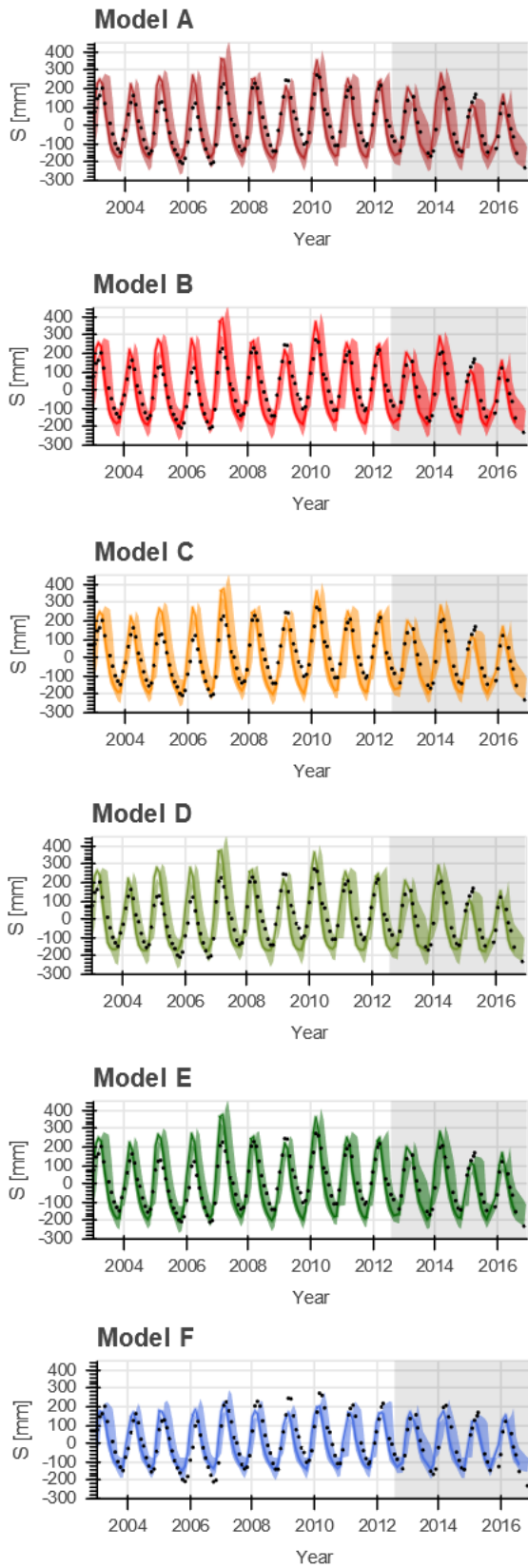


Figure S5: Range of model solutions for Models A to F. Each panel shows the time series of the recorded (black) and modelled basin average total water storage: the line indicates the solution with the highest calibration objective function with respect to discharge ($D_{E,Q_{cal}}$) and the shaded area the envelope of the solutions retained as feasible. The data in the grey shaded area were used for validation.

S2.5. Spatial pattern: Evaporation (normalised, dry season)

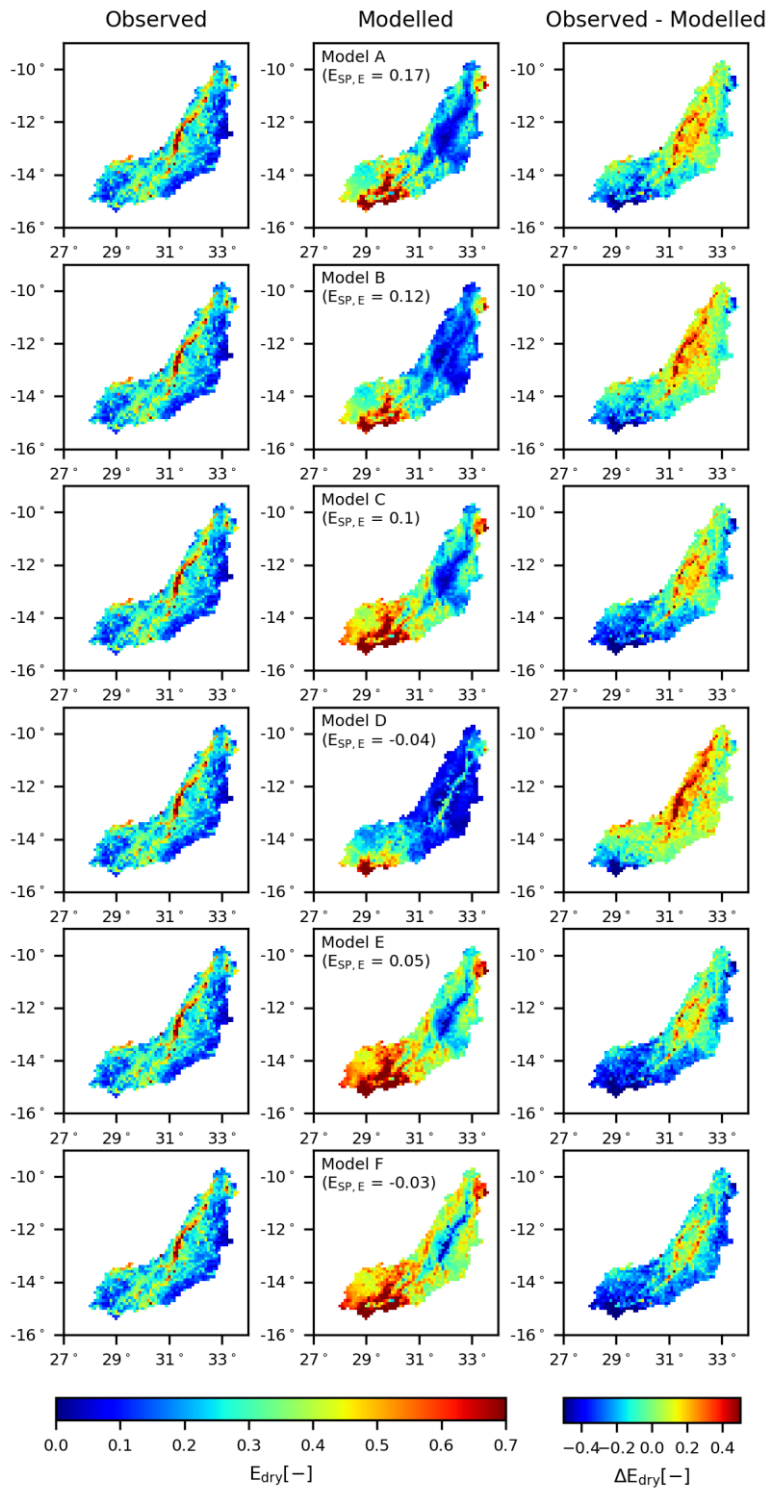


Figure S6: Spatial variability of the normalised total evaporation for Models A to F averaged over all dry seasons. The left panel shows the observation according to WaPOR data; the middle panel the model result using the “optimal” parameter set with respect to discharge ($D_{E,Q_{eal}}$); and the right panel the difference between the observation and model.

S2.6. Spatial pattern: Total water storage (normalised, dry season)

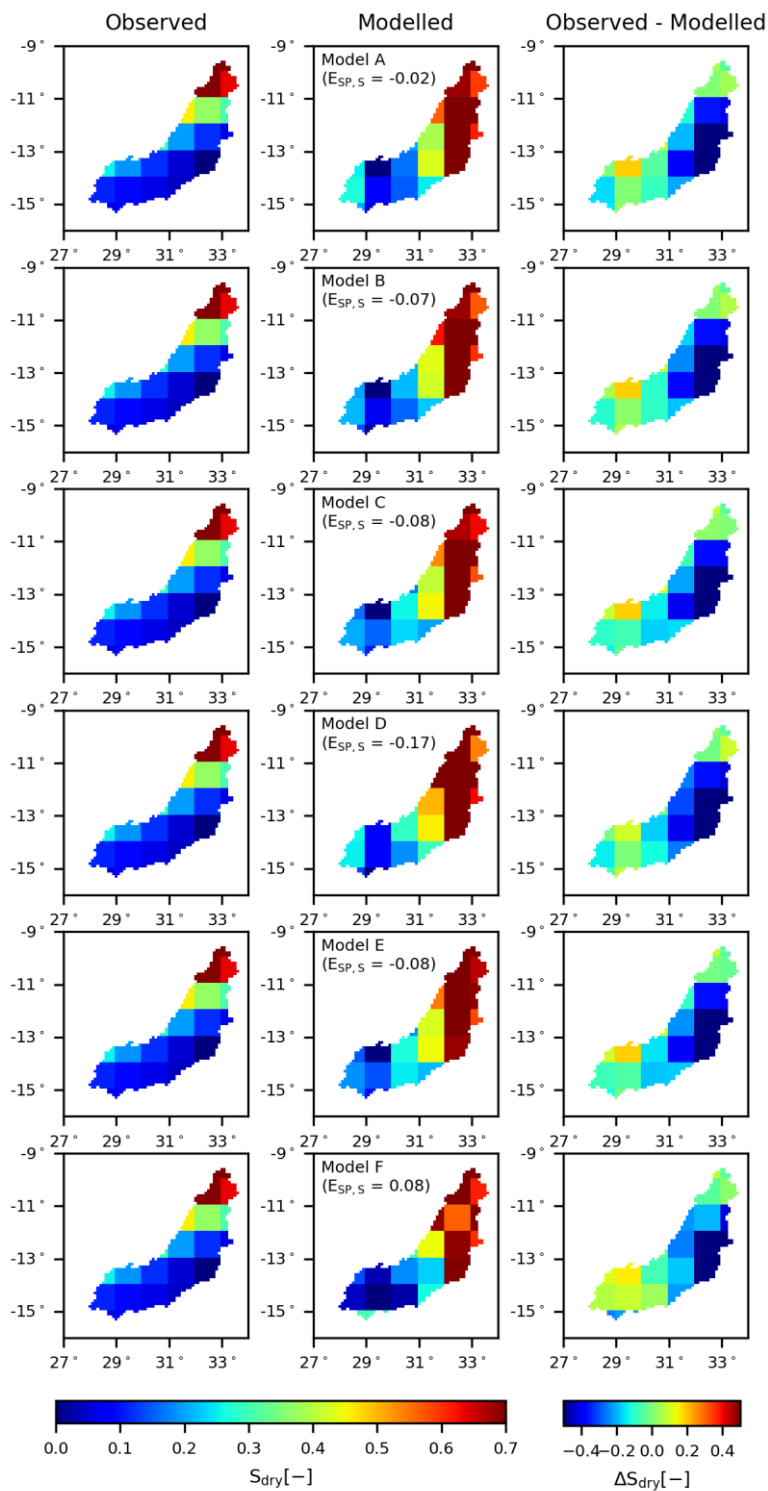


Figure S7: Spatial variability of the normalised total water storage for Models A to F averaged over all dry seasons. The left panel shows the observation according to GRACE data; the middle panel the model result using the “optimal” parameter set with respect to discharge ($D_{E,Qcal}$); and the right panel the difference between the observation and model.

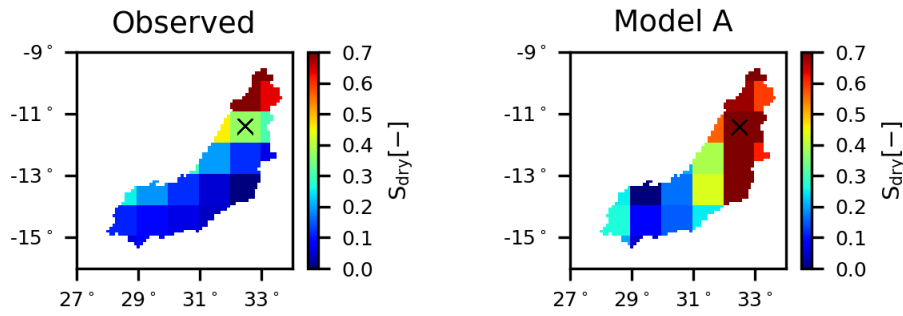


Figure S8: Spatial variability of the *normalised* total water storage anomalies for Model A averaged over all days within the dry season. The left panel shows the observation according to GRACE data, and the right panel the model result using the “optimal” parameter set with respect to discharge ($D_{E,Qcal}$).

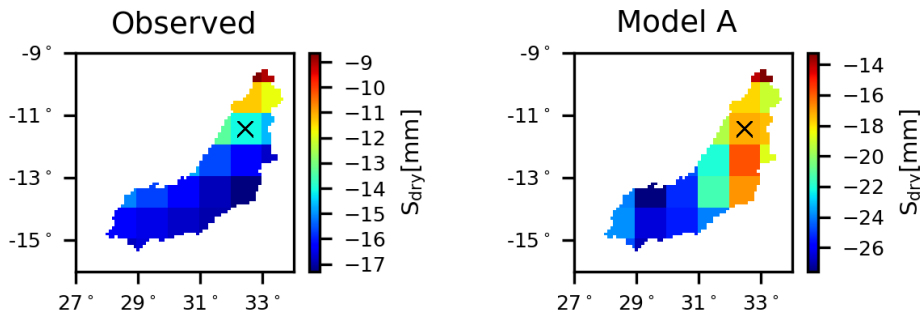


Figure S9: Spatial variability of the total water storage anomalies (*not normalised*) for Model A averaged over all days within the dry season. The left panel shows the observation according to GRACE data, and the right panel the model result using the “optimal” parameter set with respect to discharge ($D_{E,Qcal}$).

S3. Parameter sets selected based on multiple variables

S3.1. Time series: Evaporation (Basin average)

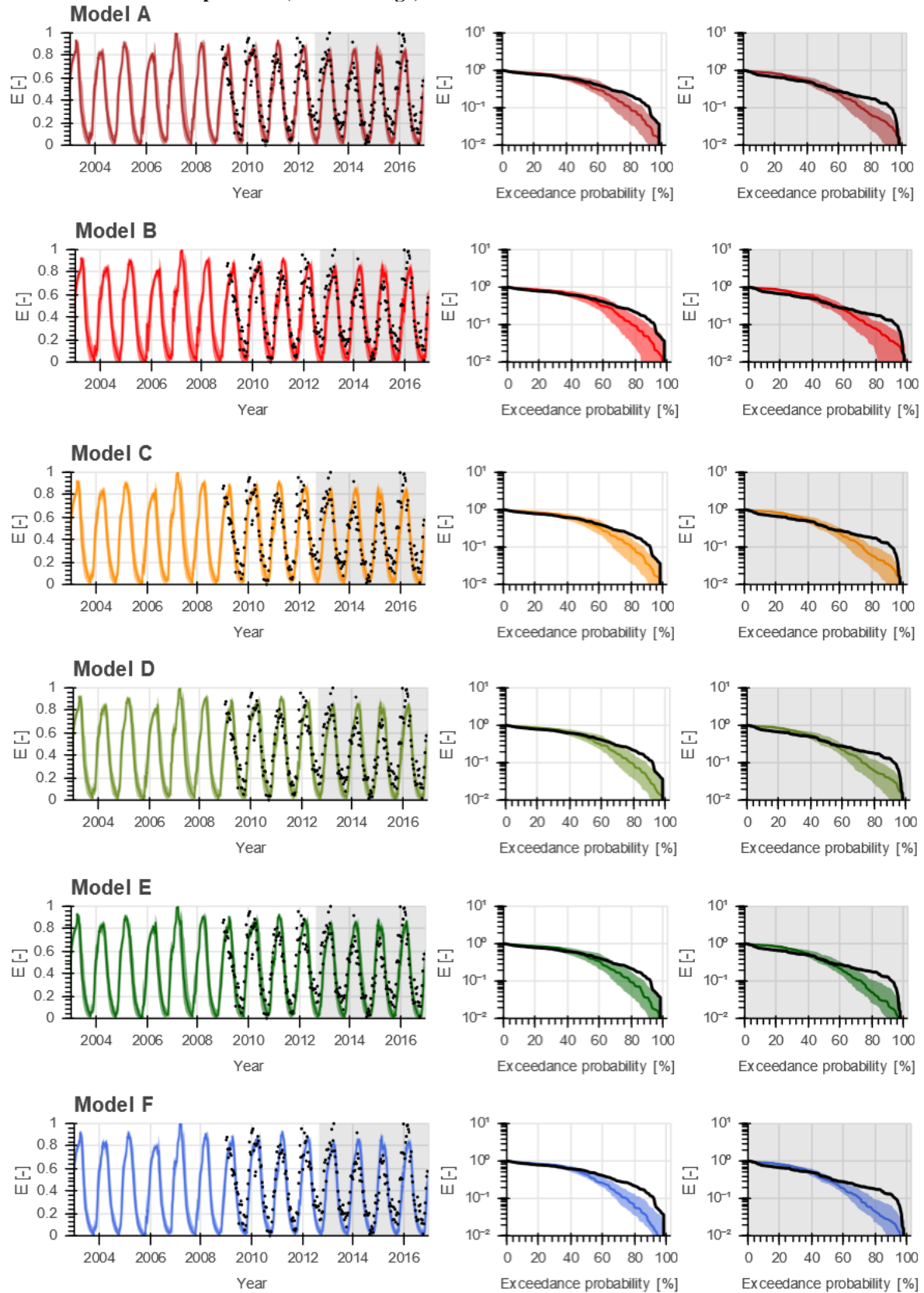


Figure S10: Range of model solutions for Models A to F. The left panel shows the time series and the right panel the duration curve of the recorded (black) and modelled normalized basin average evaporation: the line indicates the solution with the highest calibration objective function with respect to multiple variables ($D_{E,ESQ}$) and the shaded area the envelope of the solutions retained as feasible. The data in the grey shaded area were used for validation.

S3.2. Time series: Total water storage (Basin average)

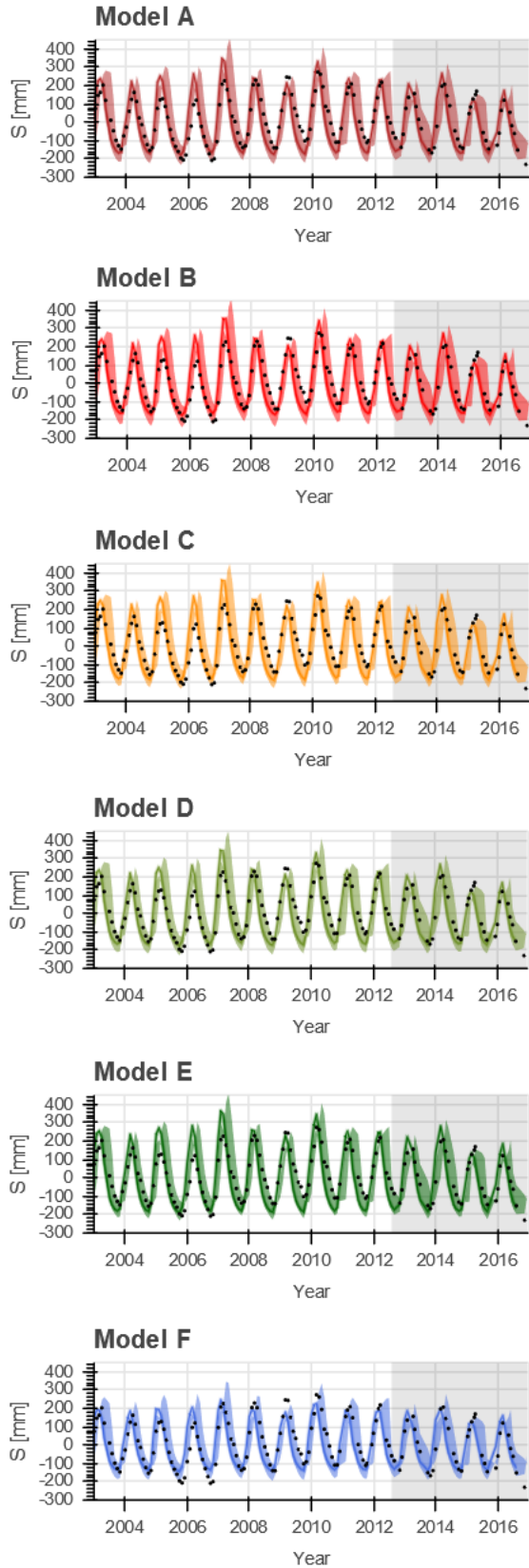


Figure S11: Range of model solutions for Models A to F. Each panel shows the time series of the recorded (black) and modelled basin average total water storage: the line indicates the solution with the highest calibration objective function with respect to multiple variables ($D_{E,ESQ}$) and the shaded area the envelope of the solutions retained as feasible. The data in the grey shaded area were used for validation

S3.3. Spatial pattern: Evaporation (normalised, dry season)

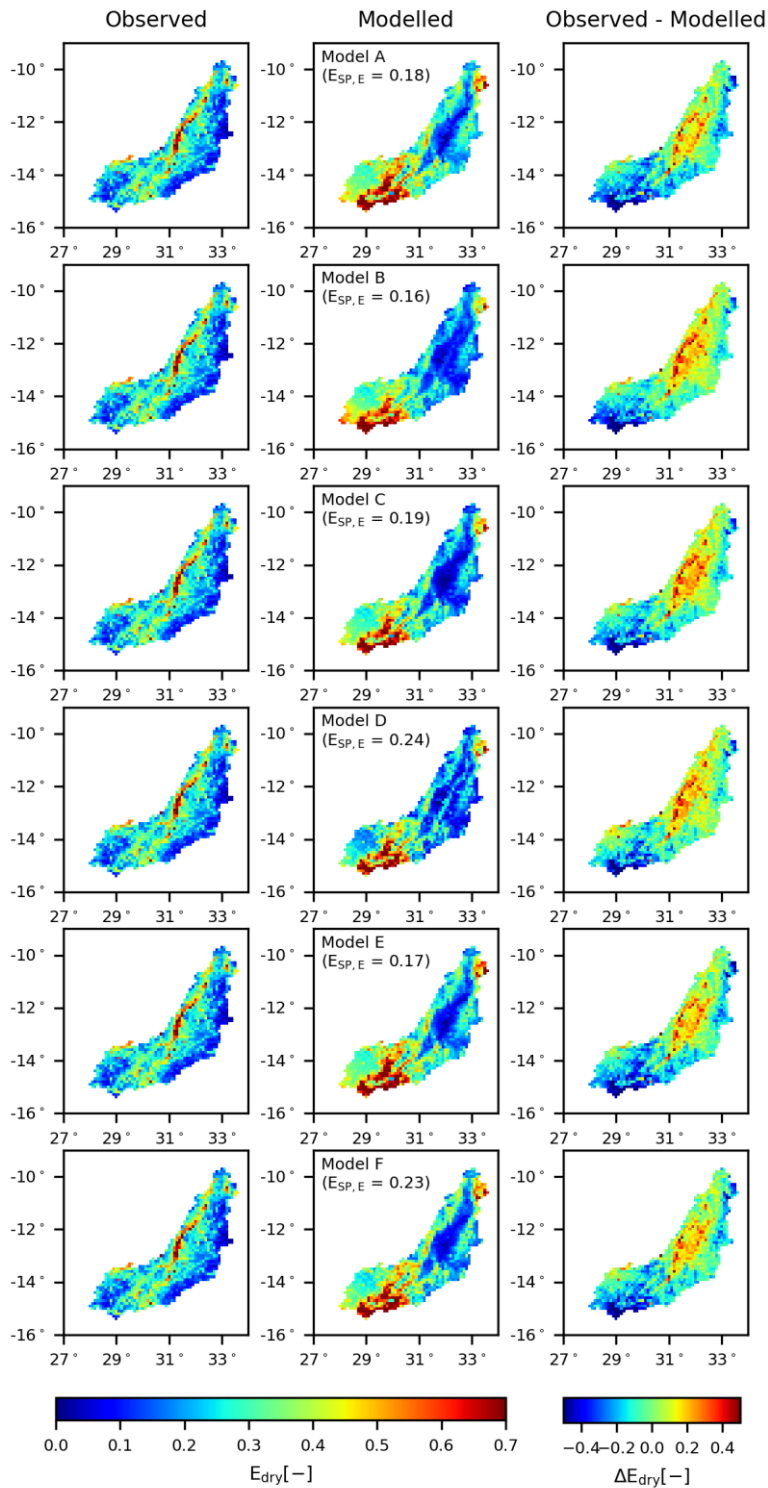


Figure S12: Spatial variability of the normalised total evaporation for Models A to F averaged over all dry seasons. The left panel shows the observation according to WaPOR data; the middle panel the model result using the “optimal” parameter set with respect to multiple variables ($D_{E,ESQ}$); and the right panel the difference between the observation and model.

S3.4. Spatial pattern: Total water storage (normalised, dry season)

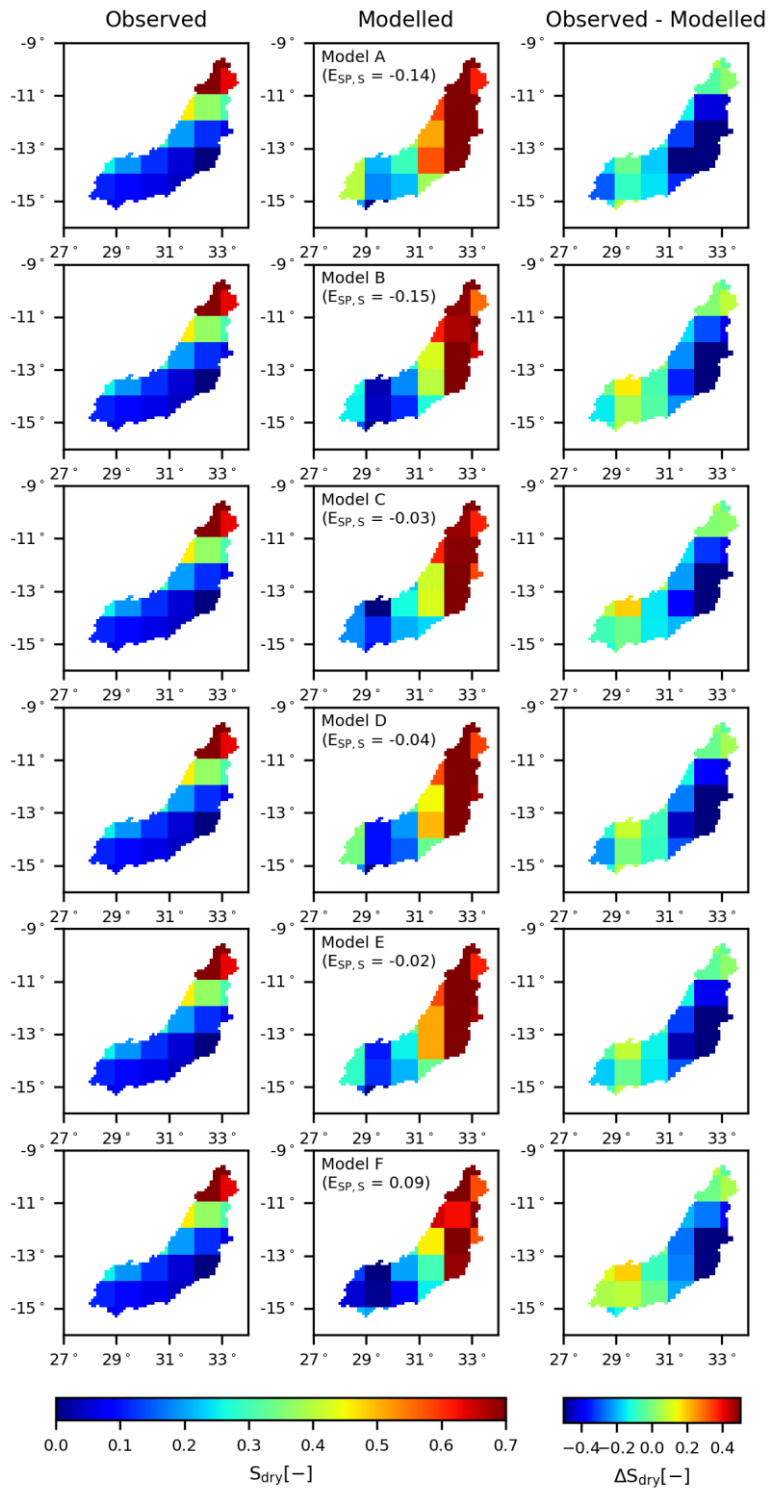


Figure S13: Spatial variability of the normalised total water storage for Models A to F averaged over all dry seasons. The left panel shows the observation according to GRACE data; the middle panel the model result using the “optimal” parameter set with respect to multiple variables ($D_{E,ESQ}$); and the right panel the difference between the observation and model.

S4. Remaining graphs

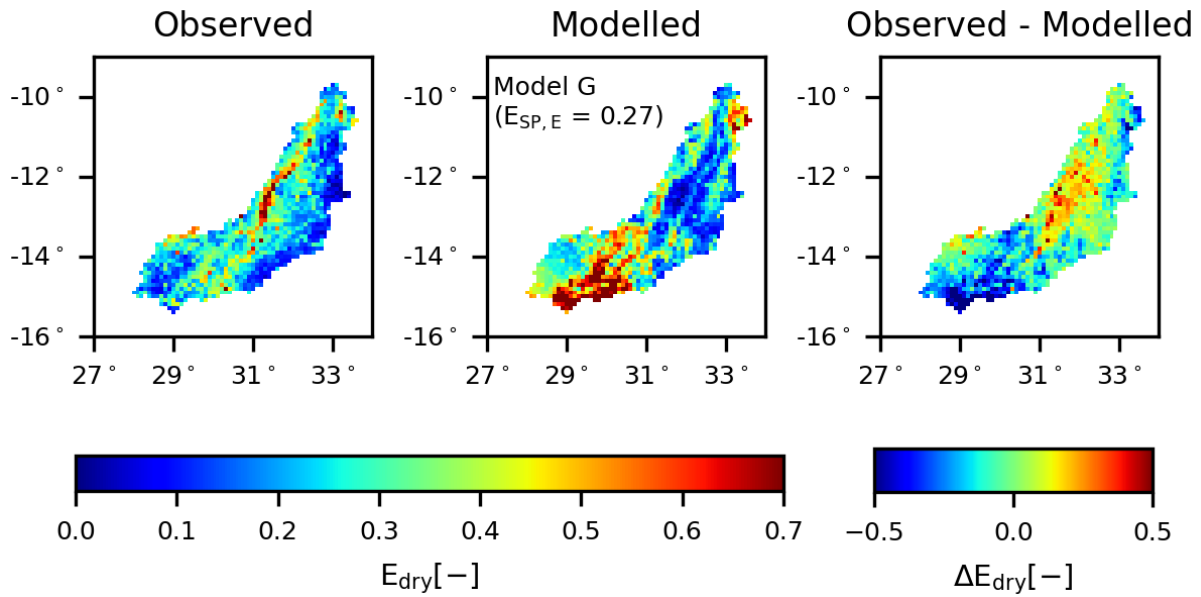


Figure S14: Spatial variability of the normalised total evaporation for Model G averaged over all days within the dry season. The left panel shows the observation according to WaPOR data, the middle panel the model result using the “optimal” parameter set with respect to multiple variables ($D_{E,ESOcal}$), and the right panel the difference between the observation and model. In Model G, the parameter I_{max} (maximum interception storage) was distributed using a linear transfer function with LAI data and using Model F as basis.

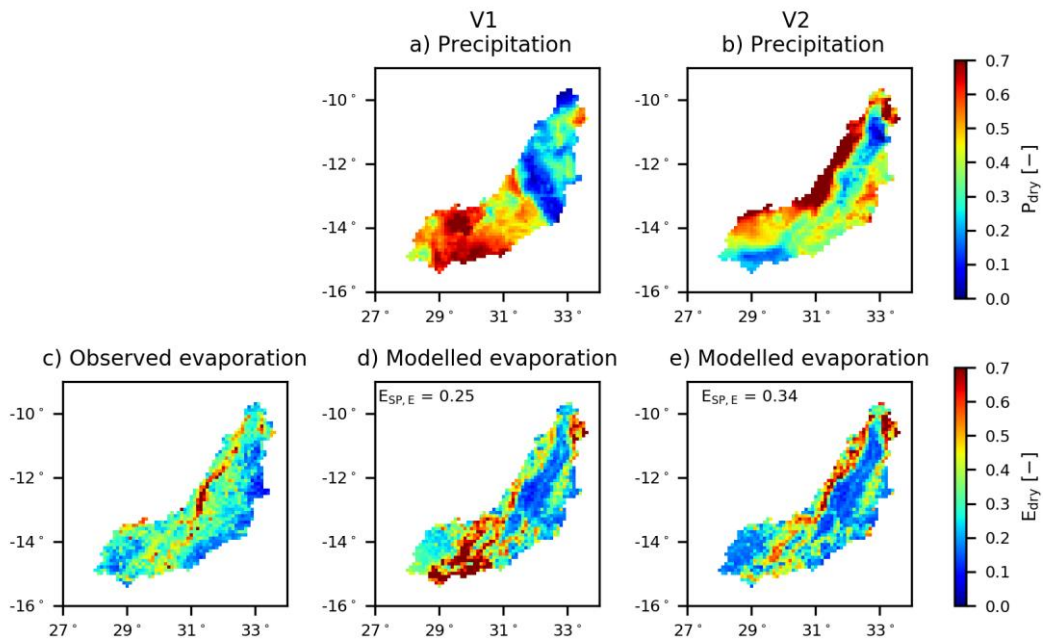


Figure S15: Effect of precipitation on the modelled evaporation for Model F using a random parameter set with a) precipitation originally used in the hydrological model (P_{V1}), b) precipitation used for WaPOR (P_{V2}), c) normalised observed evaporation according to WaPOR, d) normalised modelled evaporation using P_{V1} , and e) P_{V2} . All sub-figures show the spatial pattern averaged over all days within the dry season.

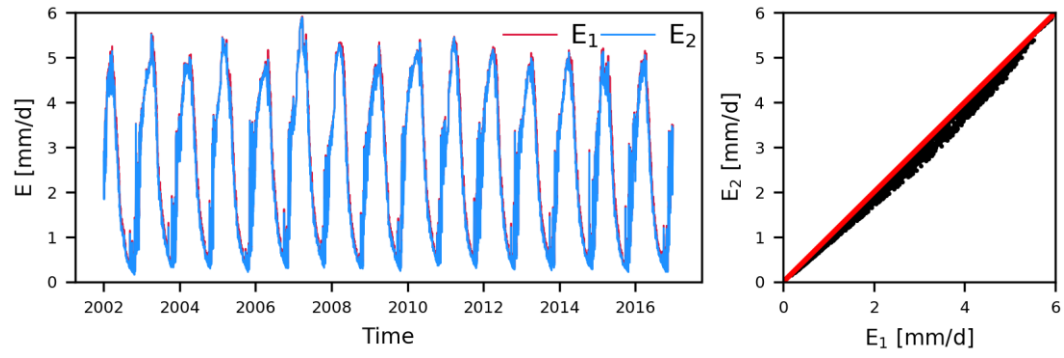


Figure S16: Modelled evaporation for one random simulation when adjusting the 1) observed evaporation (corresponding to E_1) resulting in $E_{NS,Basin,E} = 0.65$, or 2) precipitation only (corresponding to E_2) to close the long term water balance resulting in $E_{NS,Basin,E} = 0.66$. The red line in the right panel indicates the 1:1 line.

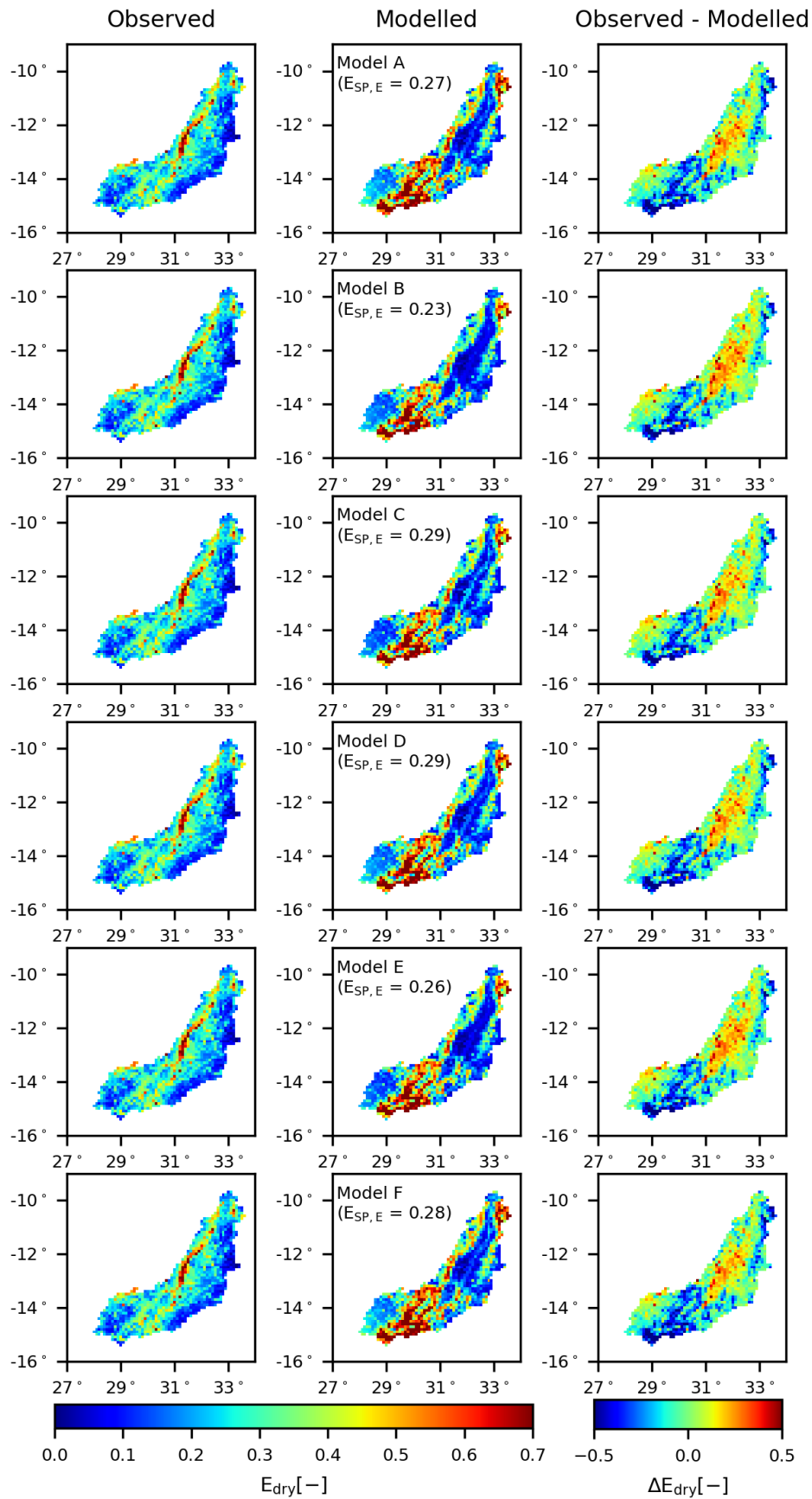


Figure S17: Spatial variability of the normalised total evaporation for Models A to F averaged over all dry seasons. The left panel shows the observation according to WaPOR data; the middle panel the model result using the “optimal” parameter set with respect to the evaporation spatial pattern ($E_{SP,E}$); and the right panel the difference between the observation and model.